# Scientific Experimentation and Evaluation

## Lab Reports: Assignments 1 & 2

**Group Members:** Jannen, Nikhil, Al Shafi

**Date:** October 2025

## Contents

# Part I

# Assignment 1: Measurement System Design

## 1 Robot and Measurement System

The robot used in this experiment is a **LEGO EV3 differential drive robot**, consisting of two main wheels on the same axle and a small supporting caster at the front. The task of the experiment is to measure the stop position of the robot after executing a predefined motion.

In the initial design, a **lever and pencil nib mechanism** was used to mark the stop position. However, it was later replaced with a **pen refill-based marking system**, which makes the system more robust for rough terrain. A pen refill is directly mounted on both sides of the robot, allowing it to make a mark on the cardboard surface. This modification simplifies the setup and improves marking consistency.

- The midpoint between the two pen marks corresponds approximately to the final position of the robot's wheel axle center.
- The orientation $\theta$ can be estimated from the line connecting the left and right marks, since they reflect the alignment of the robot's axle.

**Reason for Two-Point Measurement:** Two points are sufficient to define the robot's axle line and its midpoint, which directly correspond to the robot's final pose on the grid. Introducing a third point would substantially increase the measurement and data processing. Performing 25 trials for each of the three motion types and using three markers would expand this to 225 individual coordinate readings. Additionally, computing the centroid of a triangular configuration manually would complicate data handling and introduce more room for error. Therefore, the two-point setup achieves the necessary accuracy while keeping the experimental process straightforward and repeatable. The midpoint position and the orientation line ensure reliable results with minimal hardware.

## 2 Measurement Process

The process for carrying out the measurements is as follows:

1. A large cardboard sheet with a printed or drawn grid is fixed to the working surface using tape, so it does not move during the experiment.
2. A clear origin is marked on the grid, including both position and orientation. To ensure repeatability, a simple placement template is used so the robot always starts from the same position and orientation.
3. The robot is placed at the start position and the program for the chosen motion (straight, left arc, or right arc) is executed.

4. When the robot comes to a stop, the pen refills on both sides can be rotated 90° to avoid the stopper and pushed down simply to mark the spot, as shown in Figure 2. If both marks are recorded, their midpoint represents the final position $(x, y)$. The line through the marks gives the orientation $\theta$.

5. The $(x, y, \theta)$ values are measured relative to the origin on the grid and recorded in a results table.

6. The robot is reset to the origin and the process is repeated at least 25 times for each type of motion.

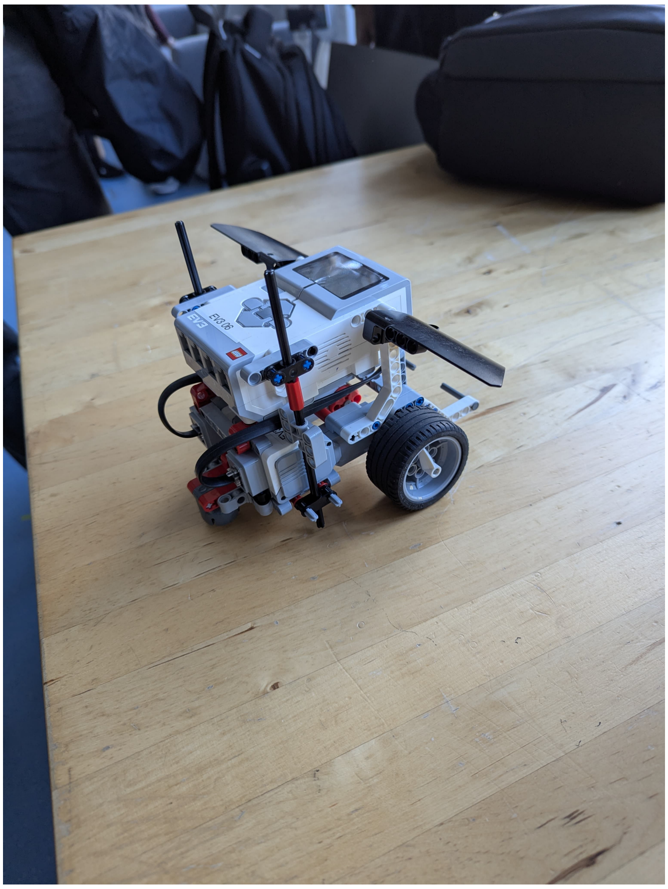

Figure 1: Robot with lever system.

# 3 Expected Problems and Mitigations

During the experiment, several practical issues may occur:

- **Ink spreading or uneven marking:** Refills may release excess ink or create faint marks. **Solution:** Use refills with consistent ink flow and test before trials.
- **Mounting stability:** If the refill is loosely mounted, mark positions may vary. **Solution:** Tape the refill to reduce any gap and improve stability.
- **Start placement variation:** Inconsistent starting positions can add systematic errors. **Solution:** Use a fixed template or taped outline for robot placement.

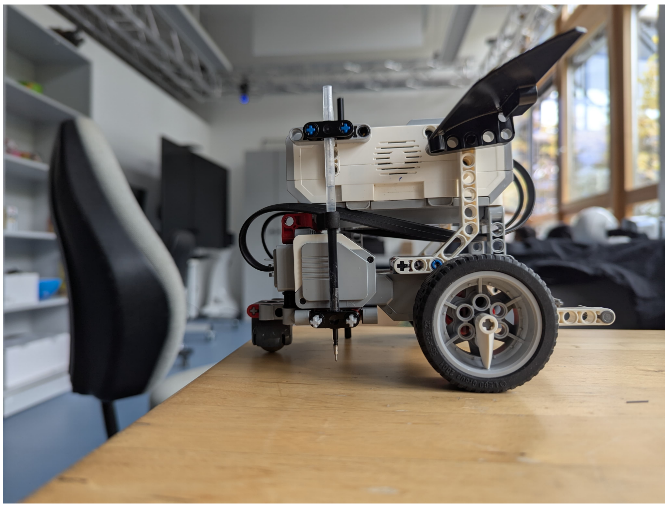

Figure 2: Robot with modified pen refill marking mechanism.

- **Cardboard movement:** If the grid sheet shifts, all measurements are affected. **Solution:** Secure the sheet with tape to the surface.

# 4 Jacobian Error Propagation

The propagation of uncertainty in the measured input coordinates requires the calculation of the Jacobian matrix $\mathbf{J}$. The total input vector $\mathbf{x} = (x_{1,1}, x_{1,2}, x_{2,1}, x_{2,2})^T$ is composed of all four scalar variables representing the coordinates of the two pen marks. Since $\mathbf{F}$ is a vector-valued function with three outputs (final pose: $x, y, \theta$) and four inputs, the resulting Jacobian matrix $\mathbf{J}$ is a $3 \times 4$ matrix.

For the orientation $\theta$, let the measured coordinates be

$$\mathbf{p} = \begin{bmatrix} x_L & y_L & x_R & y_R \end{bmatrix}^\top,$$

where the robot orientation is computed as

$$\theta(\mathbf{p}) = \operatorname{atan2}(y_R - y_L, x_R - x_L).$$

The Jacobian for orientation is given by:

$$\mathbf{J}_\theta = \frac{\partial \mathbf{F}}{\partial \mathbf{x}} = \begin{pmatrix} \frac{\partial F_1}{\partial x_{1,1}} & \frac{\partial F_1}{\partial x_{1,2}} & \frac{\partial F_1}{\partial x_{2,1}} & \frac{\partial F_1}{\partial x_{2,2}} \\ \frac{\partial F_2}{\partial x_{1,1}} & \frac{\partial F_2}{\partial x_{1,2}} & \frac{\partial F_2}{\partial x_{2,1}} & \frac{\partial F_2}{\partial x_{2,2}} \\ \frac{\partial F_3}{\partial x_{1,1}} & \frac{\partial F_3}{\partial x_{1,2}} & \frac{\partial F_3}{\partial x_{2,1}} & \frac{\partial F_3}{\partial x_{2,2}} \end{pmatrix}$$

For the third row (orientation), with $d = (x_{1,1} - x_{2,1})^2 + (x_{1,2} - x_{2,2})^2$:

$$= \begin{pmatrix} \frac{1}{2} & 0 & \frac{1}{2} & 0 \\ 0 & \frac{1}{2} & 0 & \frac{1}{2} \\ \frac{x_{1,2}-x_{2,2}}{d} & \frac{x_{2,1}-x_{1,1}}{d} & \frac{x_{2,2}-x_{1,2}}{d} & \frac{x_{1,1}-x_{2,1}}{d} \end{pmatrix}$$

The covariance matrix of the calculated end pose $\mathbf{C}_F$ is then determined from the input covariance matrix $\mathbf{C}_x$ via the generalized error propagation formula:

$$\mathbf{C}_F = \mathbf{J}\mathbf{C}_x\mathbf{J}^T, \tag{1}$$

where $\mathbf{C}_x$ is the $4 \times 4$ covariance matrix of the input variables $(x_{1,1}, x_{1,2}, x_{2,1}, x_{2,2})$.

Using the reported position uncertainty $\sigma_{\text{pos}} \approx 0.36$ mm and wheel-axle separation $L \approx 96$ mm, the orientation uncertainty is approximately:

$$\boxed{\sigma_\theta \approx 0.0053 \text{ rad} \approx 0.30^\circ}$$

# 5 Conclusion

This measurement system provides a simple, reliable, and precise method for determining the robot's final position and orientation. The direct contact of the refill with the surface ensures consistent marking with minimal error, reducing variability in results. Its compact design minimizes mechanical complexity and allows easy alignment on both sides of the robot. Due to the fine tip of the pen refill, the marking precision is high, resulting in a position uncertainty of approximately $\pm 0.4$ mm and an orientation uncertainty of about $\pm 0.2^\circ$.

Among the possible configurations, the two-point method proved to be the most straightforward and practical choice, as it provides all required position and orientation information without unnecessary complexity or excessive data recording.

# Part II

# Assignment 2: Manual Motion Observation

## 1 Introduction

This report presents the execution and results of Assignment 2, where we conducted manual measurements of our LEGO EV3 differential drive robot's end poses across three different motion types: straight, left arc, and right arc. Each motion was repeated 25 times to gather statistical data on the robot's behavior and positioning accuracy.

## 2 Program and Parameters

The robot was controlled using the provided EV3 control program with the following predefined parameters:

- **Wheel diameter:** 5.30 cm
- **Distance between wheels:** 12.00 cm
- **Pen refill offset X:** 5.50 cm
- **Pen refill offset Y:** 6.40 cm
- **Motion types:** Left arc, Straight line, Right arc
- **Trials per motion:** 25 trials each (75 total)

## 3 Observations During Execution

During the experimental runs, the following observations were made:

1. **Surface consistency:** The cardboard surface remained stable throughout all trials, providing a reliable measurement platform.
2. **Marking precision:** The pen refill mechanism produced consistent marks with minimal ink spreading. The fine tip allowed for precise position recording.
3. **Start position repeatability:** Using a fixed template ensured consistent starting positions across all trials, minimizing systematic errors.
4. **Robot behavior variations:** Slight variations in end positions were observed, likely due to:
    - Motor encoder resolution limitations
    - Battery voltage variations affecting motor performance
    - Minor inconsistencies in floor levelness

5. **Motion characteristics:**
   - *Straight motion:* Generally consistent forward movement.
   - *Left arc:* Smooth curved trajectory with good repeatability
   - *Right arc:* Similar behavior to left arc, symmetric results observed

# 4 Data Collection and Transformation

The experiment was conducted on a large cardboard sheet with a printed grid, which served as the global coordinate frame. A fixed starting pose was used for all trials to ensure consistency.

For each of the 25 runs per motion (left arc, straight, right arc), the following procedure was followed:

- The robot was placed at the designated origin (0, 0).
- The corresponding motion program was executed.
- Upon stopping, the two pen refills were used to mark the robot's position.
- The coordinates of the two marks, $(X1, Y1)$ and $(X2, Y2)$, were recorded.

The raw marker coordinates were then transformed to calculate the final pose of the wheel axle center. This involved a three-step mathematical process:

1. **Midpoint Calculation:** The midpoint of the pen refills, (Avg X, Avg Y), was found by averaging the coordinates:

   $$\mathrm{X} = \frac{X1 + X2}{2}, \quad \mathrm{Y} = \frac{Y1 + Y2}{2}$$

2. **Orientation Calculation:** The final orientation, $\theta$, was calculated based on the position of the robot's axle center. By convention, an orientation of $\theta = 0$ corresponds to the robot facing along the positive Y-axis.

   The radius of curvature is:

   $$r = \frac{X^2 + Y^2}{2X}$$

   The orientation angle $\theta$ is defined as:

   $$\theta = \arctan \frac{Y2 - Y1}{X2 - X1}$$

   Finally, the orientation is rounded to two decimal places:

   $$\theta_{\text{final}} = \text{round}(\theta, 2)$$

# 5 Data Visualization

The collected data has been visualized in three comprehensive plots showing the robot's behavior for each motion type. The visualizations include both the manually measured end poses and the complete paths recorded by the encoder data.

## 5.1 Manual Markings on Paper

Figure 3 presents the markings of robot position.

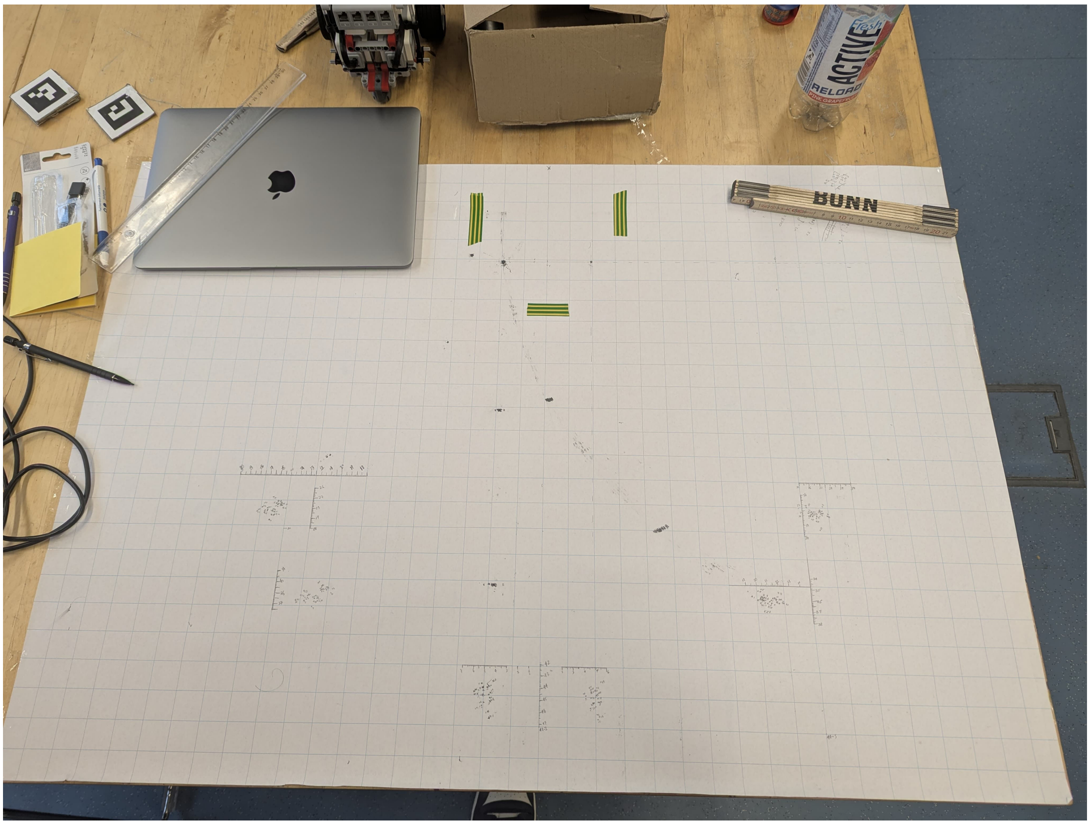


Figure 3: Manual Measurements and markings for each run of robot

## 5.2 End Poses Visualization

Figure 4 shows the distribution of the robot's end poses for all three motion types from the manual measurements. This plot illustrates the spread and clustering of final positions, providing insight into the precision of the robot's motion control.

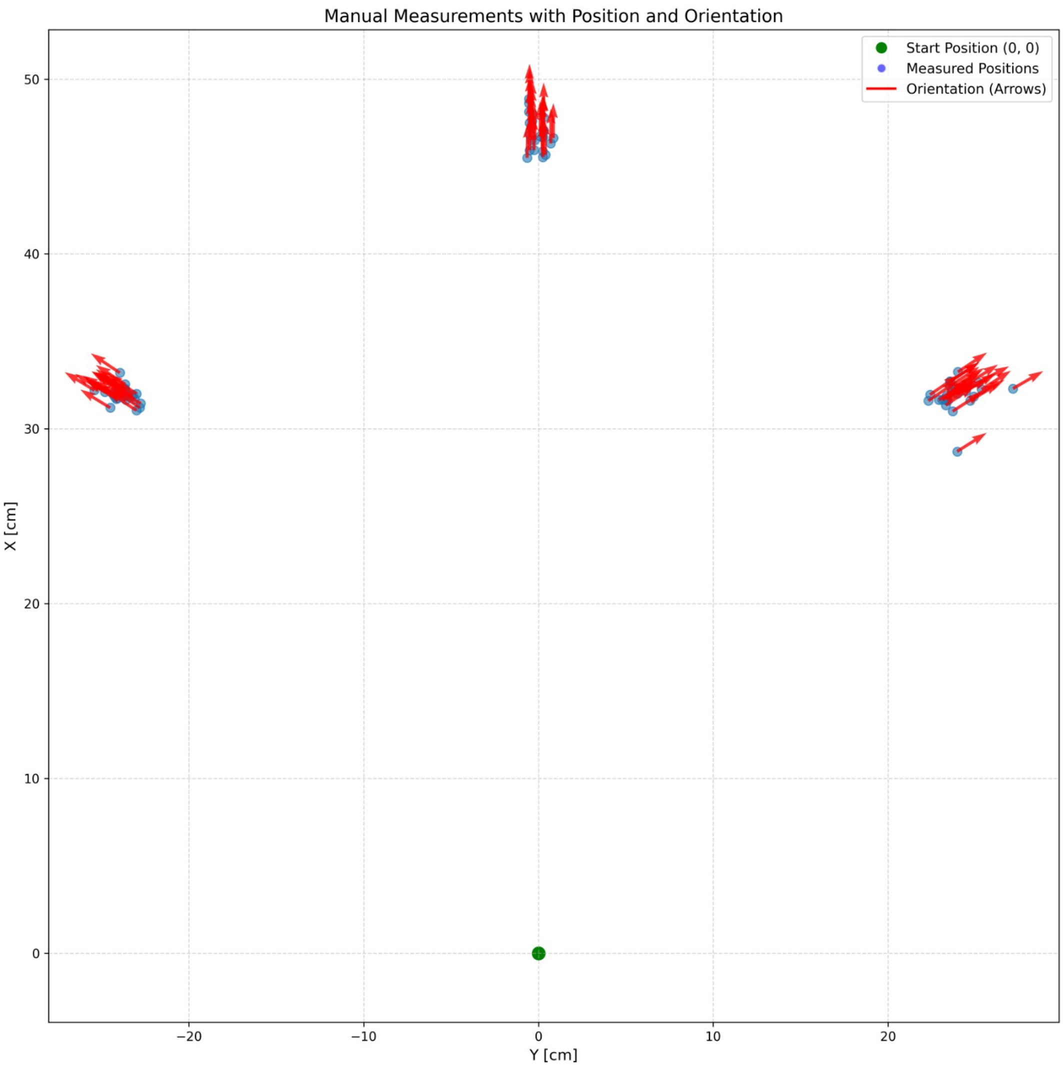


Figure 4: Robot end poses from manual measurements for straight, left arc, and right arc motions. Each point represents the compensated midpoint position between the two pen marks after refill offset correction.

## 5.3 Complete Robot Paths

Figure 5 displays the complete trajectories of the robot as recorded by the encoder measurements. This visualization shows the continuous path taken by the robot from start to finish for all trials.

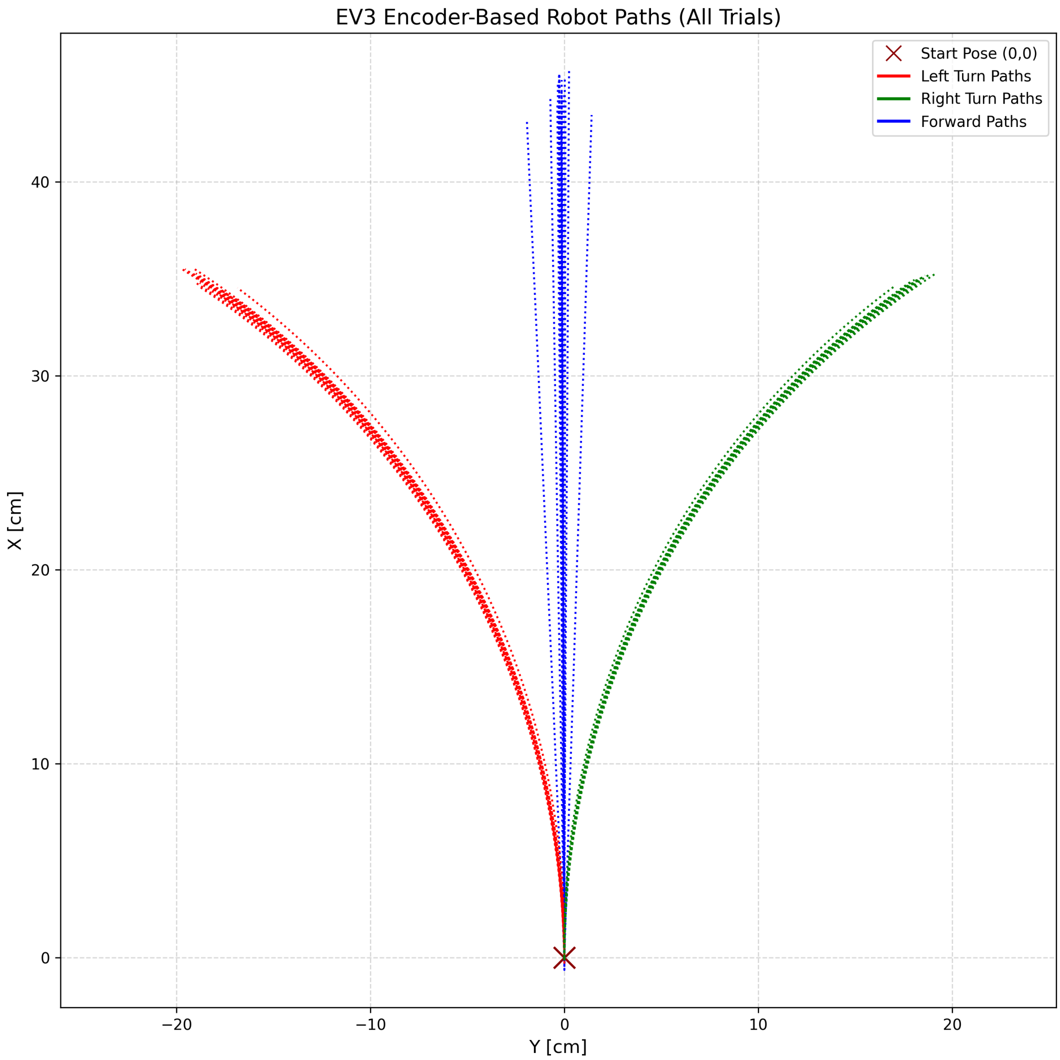


Figure 5: Complete robot paths from encoder measurements showing the trajectories for all three motion types. The paths demonstrate the robot's movement behavior from the starting pose to the final positions.

## 5.4 Combined Visualization

Figure 6 presents a combined view that overlays the manually measured end poses with the encoder-based path data, allowing for direct comparison between the two measurement methods.

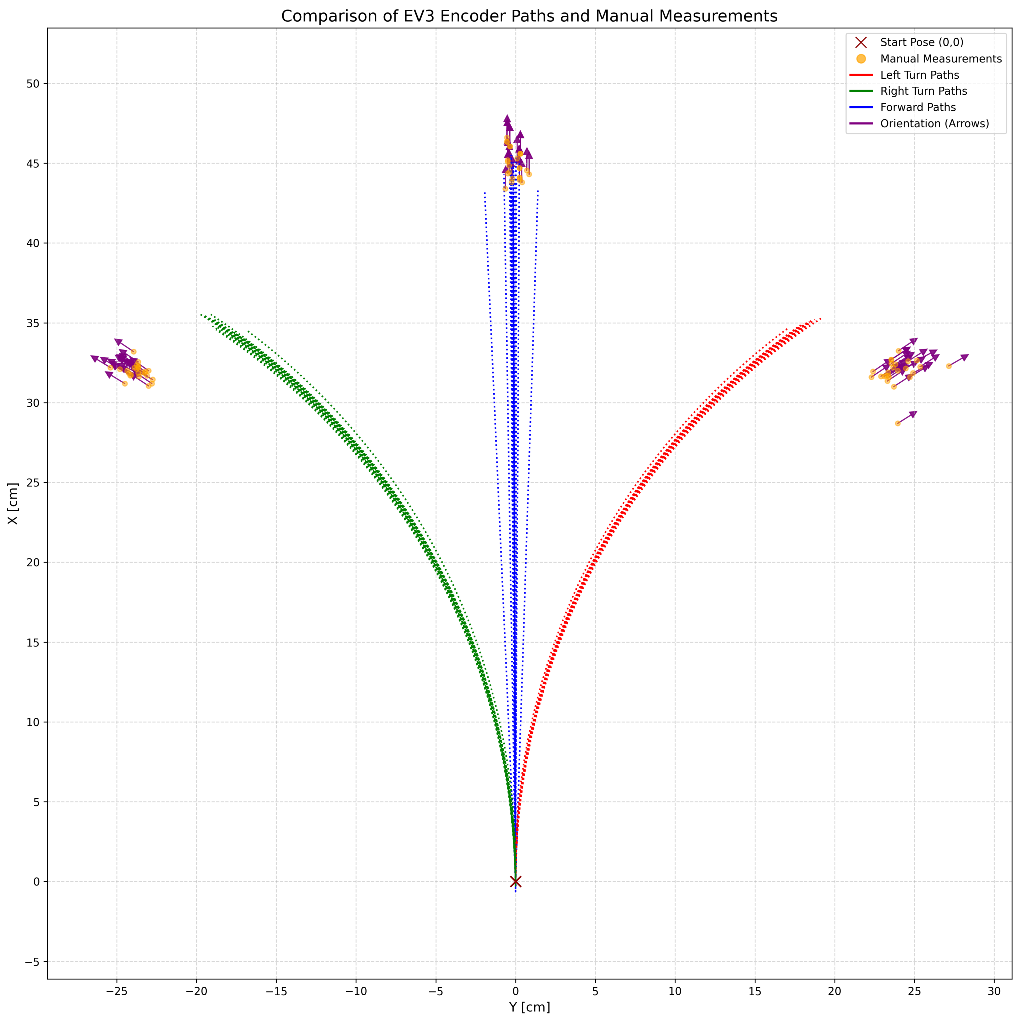


Figure 6: Combined visualization showing both encoder-based paths and manually measured end poses. This allows for comparison between the internal sensor data and external measurements.

## 5.5 Combined Visualization of All Groups

Figure 7 presents a combined view of data taken from other groups.

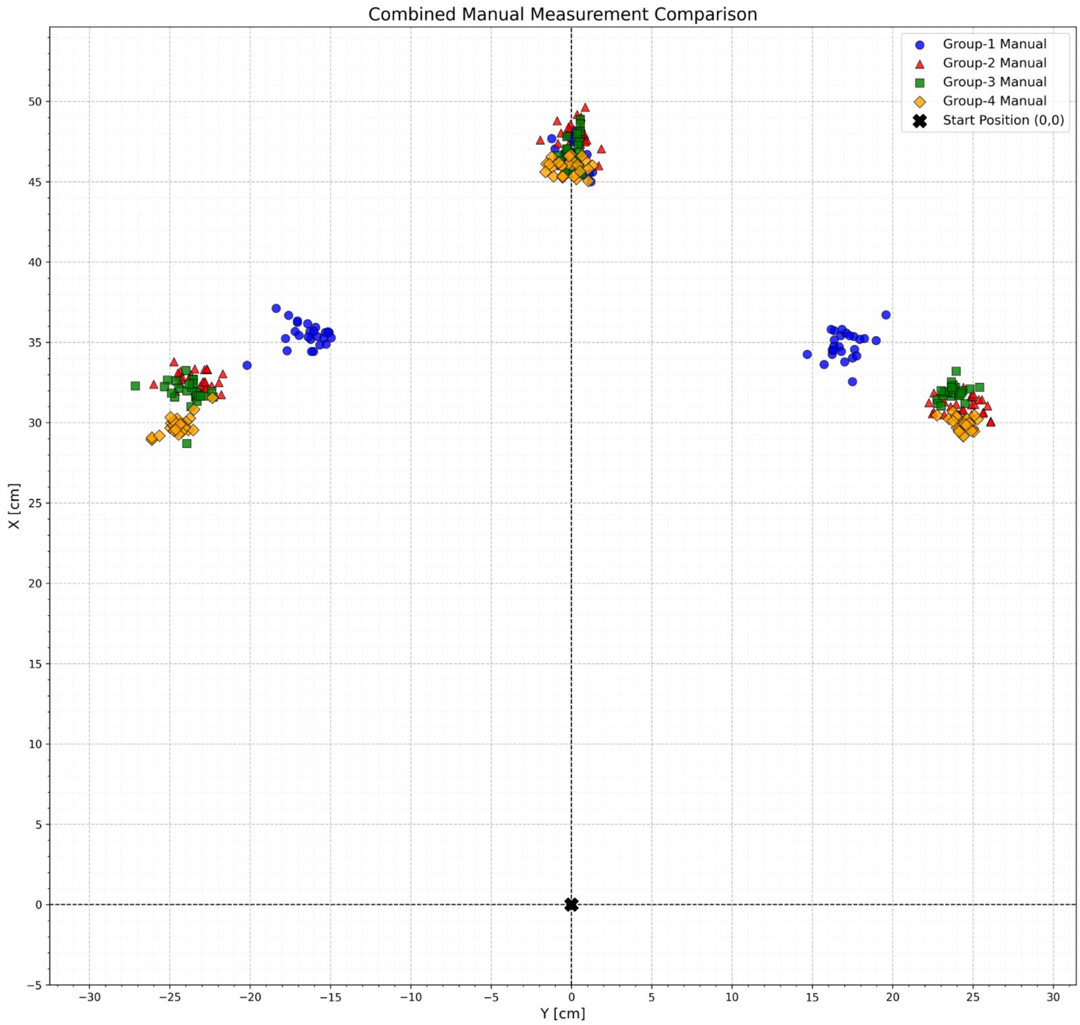


Figure 7: Combined visualization showing manually measured end poses from other groups and comparing with our group.

## 5.6 Combined Visualization of Trajectories

Figure 8 presents a combined view of data taken from other groups.

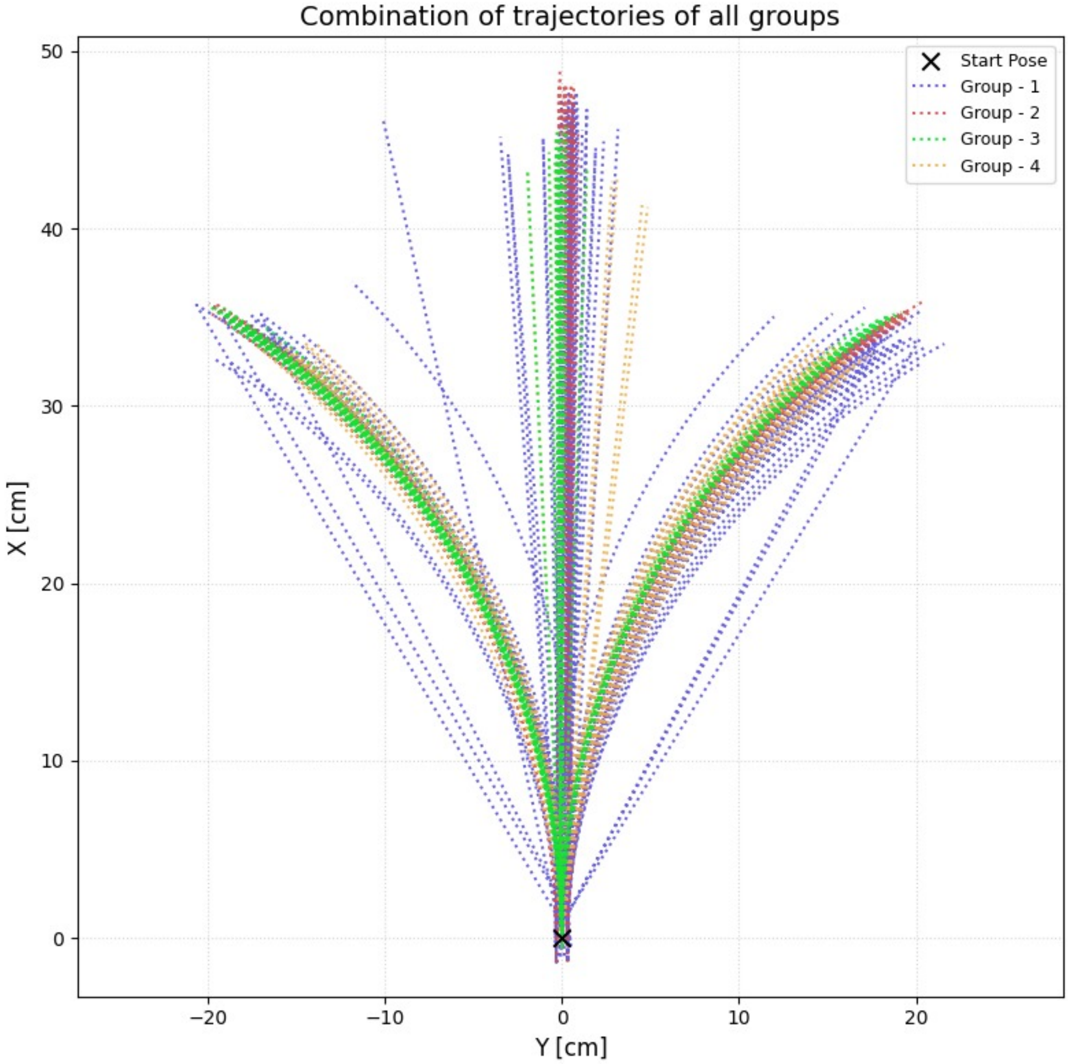


Figure 8: Combined visualization showing encoder data from other groups and comparing with our group.

# 6 Manual Measurement Data

The following sections present the complete raw measurement data collected during the experiment. All measurements are relative to the fixed coordinate system established on the grid-lined cardboard sheet, with the Y-axis aligned with the robot's initial forward direction and the X-axis perpendicular to it (following the right-hand rule).

## 6.1 Straight Motion Data

Table 1: Straight Motion - Manual Measurements (All values in cm, orientation in degrees)

| **Trial** | **x** | **y** | $\theta$ |
|---|---|---|---|
| 1 | 47.03 | 0.30 | 0.00 |
| 2 | 45.87 | 0.25 | -0.59 |
| 3 | 45.54 | 0.25 | -2.36 |
| 4 | 47.01 | 0.25 | -1.18 |
| 5 | 45.67 | 0.40 | -1.19 |
| 6 | 45.94 | -0.25 | -1.18 |
| 7 | 47.61 | -0.35 | -0.59 |
| 8 | 47.50 | -0.50 | 0.00 |
| 9 | 47.25 | -0.40 | 0.60 |
| 10 | 46.52 | -0.20 | -0.60 |
| 11 | 46.71 | 0.25 | -1.18 |
| 12 | 48.88 | -0.55 | 1.21 |
| 13 | 48.61 | -0.55 | 1.77 |
| 14 | 46.73 | 0.10 | 0.00 |
| 15 | 46.50 | -0.40 | -0.61 |
| 16 | 46.63 | 0.85 | 0.00 |
| 17 | 45.93 | -0.50 | 0.60 |
| 18 | 46.84 | -0.50 | 1.19 |
| 19 | 45.50 | -0.65 | 1.21 |
| 20 | 47.81 | 0.30 | 0.00 |
| 21 | 46.32 | 0.70 | 0.58 |
| 22 | 48.14 | -0.55 | 1.77 |
| 23 | 48.01 | -0.35 | -0.59 |
| 24 | 46.67 | 0.25 | -2.36 |
| 25 | 47.06 | 0.30 | 0.00 |

## 6.2 Left Arc Motion Data

Table 2: Left Arc Motion - Manual Measurements (All values in cm, orientation in degrees)

| **Trial** | **x(cm)** | **y(cm)** | $\theta$**(deg)** |
|---|---|---|---|
| 1 | 31.45 | -22.75 | -62.10 |
| 2 | 31.65 | -23.60 | -62.59 |
| 3 | 31.85 | -23.65 | -64.29 |
| 4 | 31.20 | -22.80 | -55.98 |
| 5 | 31.05 | -23.00 | -56.65 |
| 6 | 31.90 | -23.40 | -56.98 |
| 7 | 31.20 | -24.50 | -58.63 |
| 8 | 31.85 | -23.25 | -57.15 |
| 9 | 31.70 | -23.10 | -55.98 |
| 10 | 31.95 | -23.20 | -57.30 |
| 11 | 32.20 | -23.90 | -56.98 |
| 12 | 32.20 | -23.65 | -60.18 |
| 13 | 32.30 | -23.65 | -56.48 |
| 14 | 32.35 | -23.75 | -62.57 |
| 15 | 32.10 | -24.80 | -58.63 |
| 16 | 32.00 | -24.35 | -58.74 |
| 17 | 31.75 | -24.10 | -58.31 |
| 18 | 31.70 | -24.15 | -58.12 |
| 19 | 32.55 | -23.65 | -56.80 |
| 20 | 32.10 | -23.75 | -56.48 |
| 21 | 32.20 | -25.40 | -58.63 |
| 22 | 32.20 | -23.65 | -60.18 |
| 23 | 33.20 | -23.95 | -56.14 |
| 24 | 31.85 | -24.25 | -57.80 |
| 25 | 32.00 | -23.00 | -55.30 |

## 6.3 Right Arc Motion Data

Table 3: Right Arc Motion - Manual Measurements (All values in cm, orientation in degrees)

| **Trial** | **x(cm)** | **y(cm)** | $\theta$**(deg)** |
|---|---|---|---|
| 1 | 32.65 | 25.15 | 62.61 |
| 2 | 31.90 | 23.35 | 56.48 |
| 3 | 31.60 | 22.30 | 55.98 |
| 4 | 31.00 | 23.70 | 56.98 |
| 5 | 31.60 | 23.40 | 56.98 |
| 6 | 31.95 | 22.40 | 55.65 |
| 7 | 31.70 | 23.35 | 57.48 |
| 8 | 31.35 | 23.30 | 56.31 |
| 9 | 31.70 | 23.20 | 59.04 |
| 10 | 32.30 | 27.15 | 60.00 |
| 11 | 32.00 | 23.95 | 66.10 |
| 12 | 33.25 | 24.00 | 56.31 |
| 13 | 32.60 | 24.60 | 57.62 |
| 14 | 28.70 | 23.95 | 57.80 |
| 15 | 31.65 | 22.90 | 56.31 |
| 16 | 32.20 | 23.65 | 56.48 |
| 17 | 31.65 | 23.10 | 58.31 |
| 18 | 32.70 | 23.55 | 56.48 |
| 19 | 32.70 | 23.55 | 56.48 |
| 20 | 32.15 | 24.45 | 59.44 |
| 21 | 32.45 | 23.55 | 56.80 |
| 22 | 32.25 | 25.35 | 57.53 |
| 23 | 31.60 | 24.70 | 58.63 |
| 24 | 31.85 | 24.90 | 61.66 |
| 25 | 32.40 | 23.80 | 57.62 |

# 7 Comparison with Expectations

The observed behavior of the robot generally matches our expectations from Assignment 1:

1. **Motion repeatability:** All three motion types show relatively tight clustering of end poses, indicating good repeatability of the robot's motion control.
2. **Systematic patterns:** The straight motion shows minimal lateral drift (mean X 0), while the left and right arcs show symmetric behavior with respect to the Y-axis, as expected.
3. **Variation sources:** The spread in end positions aligns with anticipated error sources including encoder resolution, wheel slippage, and battery variations.

# 8 Data Transformation and Combined Dataset

Our data follows the standard coordinate convention agreed upon by all groups:

- X-axis aligned with forward robot direction
- Y-axis perpendicular (right-hand rule)
- All positions transformed to represent the robot's axle center
- All values rounded to 2 decimal places

# 9 Conclusion

The experiment successfully captured 75 data points (25 trials $\times$ 3 motion types) documenting the robot's end pose behavior. The pen refill marking mechanism proved reliable and precise, and the observed motion patterns demonstrate good repeatability. The visualizations clearly show the distribution of end poses and provide insight into the robot's motion characteristics.

The comparison between manually measured end poses and encoder-based trajectories reveals the strengths and limitations of both measurement approaches. The manual measurements provide ground truth data for the robot's final position, while the encoder data captures the complete motion trajectory.

# 10 Appendix: Video Documentation

Three video recordings were captured showing the robot's behavior during the experiment:

- `straight_motion.mp4` - Robot executing straight line motion
- `left_motion.mp4` - Robot executing left motion
- `right_arc_motion.mp4` - Robot executing right arc motion